

Accepted Manuscript

Research paper

Modifying the steric and electronic character within Re(I)-phenanthroline complexes for electrocatalytic CO₂ reduction

Bertrand J. Neyhouse, Travis A. White

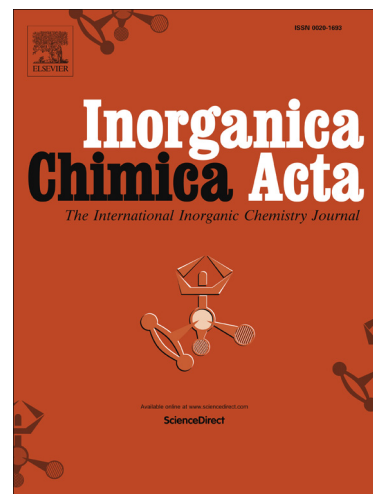
PII: S0020-1693(18)30066-5
DOI: <https://doi.org/10.1016/j.ica.2018.04.008>
Reference: ICA 18199

To appear in: *Inorganica Chimica Acta*

Received Date: 15 January 2018
Revised Date: 5 April 2018
Accepted Date: 6 April 2018

Please cite this article as: B.J. Neyhouse, T.A. White, Modifying the steric and electronic character within Re(I)-phenanthroline complexes for electrocatalytic CO₂ reduction, *Inorganica Chimica Acta* (2018), doi: <https://doi.org/10.1016/j.ica.2018.04.008>

This is a PDF file of an unedited manuscript that has been accepted for publication. As a service to our customers we are providing this early version of the manuscript. The manuscript will undergo copyediting, typesetting, and review of the resulting proof before it is published in its final form. Please note that during the production process errors may be discovered which could affect the content, and all legal disclaimers that apply to the journal pertain.



Modifying the steric and electronic character within Re(I)-phenanthroline complexes for electrocatalytic CO₂ reduction

*Bertrand J. Neyhouse and Travis A. White**

*Department of Chemistry and Biochemistry, Clippinger Laboratories, Ohio
University, Athens, Ohio 45701, United States*

Abstract: We have synthesized and characterized a series of *fac*-[Re(R₂phen)(CO)₃Cl] complexes (R₂phen = 2,9-disubstituted-1,10-phenanthroline) that function as electrocatalysts for the reduction of CO₂ to CO. The 2,9-disubstituted phenanthroline ligands contain proton (**phen**), methyl (**2,9-Me₂phen**), trimethylphenyl (**Mes₂phen**), or trimethoxyphenyl (**((2,4,6-tmp)₂phen** and **(3,4,5-tmp)₂phen**) groups as steric and electronic modifiers to provide insight into factors impacting catalytic activity. Cyclic voltammograms (CVs) recorded in CO₂-saturated CH₃CN or DMF solutions reveal that following two-electron reduction and chloride dissociation to form the active [Re(R₂phen)(CO)₃]⁻ intermediate, current enhancement indicative of CO₂ reduction to CO was observed and confirmed by controlled potential electrolysis (CPE). Using current enhancement values (i_{cat}/i_p , where i_{cat} and i_p are the current response under CO₂ and N₂, respectively) to estimate catalytic activity, it was observed that catalysts with more cathodic Re^{I/0} potentials displayed greater activity, in accord with an electronic effect driving catalysis.

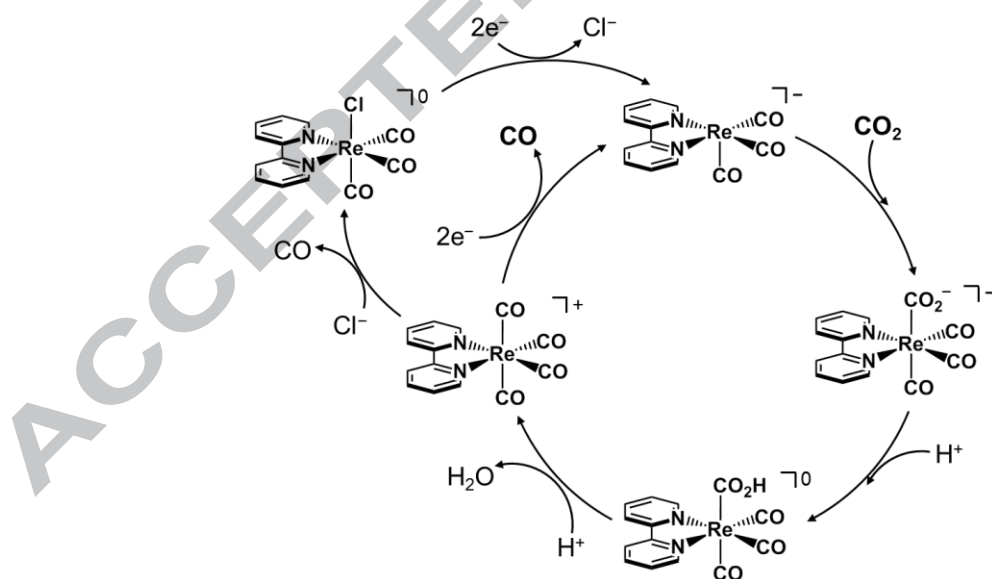
Interestingly, the trimethoxyphenyl-substituted complexes **Re((2,4,6-tmp)₂phen)** and **Re((3,4,5-tmp)₂phen)** showed different degrees of activity in DMF ($i_{cat}/i_p = 14.8$ and 6.0 , respectively) and CH₃CN ($i_{cat}/i_p = 8.5$ and 7.7 , respectively). These results suggest that while electronics dominate the observed catalytic activity within this *fac*-[Re(R₂phen)(CO)₃Cl] architecture, factors such as sterics and solvent play an important role as well.

Keywords: electrocatalytic CO₂ reduction, rhenium(I) catalyst, phenanthroline, sterics, electronics

1. Introduction

Carbon dioxide is a thermodynamically stable, kinetically inert product of carbon-based fuel combustion that can serve as a raw material to produce high-value commodities [1, 2]. CO₂ reduction products such as carbon monoxide (CO) and formic acid (HCOOH) are valuable compounds; CO is a starting material in the Fischer-Tropsch process to produce synthetic fuels and HCOOH has been proposed as a method for storing hydrogen (H₂) fuel in the liquid phase. Given the energetically-demanding nature for the 1e⁻ reduction of CO₂ to form the CO₂^{-•} radical anion ($E^{0'} = -1.90$ V vs. NHE, pH = 7, 25 °C), accessing the 2e⁻/2H⁺ reduction pathway provides a more thermodynamically accessible route to produce CO ($E^{0'} = -0.53$ V vs. NHE) [2]. Molecular electrocatalysts are attractive options given the ability to fine-tune the steric and electronic environment surrounding the catalytically-active center with the aim of producing rapid and selective catalysts [2-7]. Furthermore, catalysts possessing multiple redox-active components can be designed to deliver multiple electrons and protons to CO₂, avoiding high-energy intermediates that may hinder catalysis.

Within the scope of molecular electrocatalysts for CO₂ reduction, several architectures have proven to be active, selective, and capable of synthetic modifications, with a few examples including tetraazamacrocycles [8-13], phosphines [14-16], and diimines [4, 17]. Early reports illustrating the selective reduction of CO₂ to CO by *fac*-[Re(bpy)(CO)₃Cl] (bpy = 2,2'-bipyridine) established the foundation for this Re(I)-NN architecture (NN = bidentate diimine ligand) to be further studied [18, 19]. Cathodic cyclic voltammograms typically result in multi-electron reduction and monodentate ligand loss (e.g. halide, CH₃CN, triflate) to afford a coordinately-unsaturated, five-coordinate [Re(NN)(CO)₃]⁻ intermediate readily available to transfer electrons to the CO₂ substrate. **Scheme 1** highlights a proposed catalytic cycle for CO₂ reduction, which proceeds *via* two-electron reduction to activate the catalyst. Multiple research groups have established the non-innocent nature of the bipyridine ligand by incorporating a range of substituents to emphasize the effect of steric and/or electronic contributions within the primary and secondary coordination spheres towards catalysis [20-28].



Scheme 1. One proposed catalytic cycle for CO₂ reduction using *fac*-[Re(diimine)(CO)₃Cl] complexes.

As shown in **Scheme 1**, the proposed catalytic cycle involves coordination of CO₂ to the five-coordinate [Re(NN)(CO)₃]⁻ intermediate to form a metallocarboxylate [Re(NN)(CO₂)(CO)₃]⁻ intermediate. The metallocarboxylate (Re-CO₂) undergoes rapid protonation to form a metallocarboxylic acid structure, [Re(NN)(CO₂H)(CO)₃] (Re-CO₂H), that can be further protonated to evolve water and a tetracarbonyl rhenium species, [Re(NN)(CO)₄]⁺ (Re-CO), prior to CO evolution [29-34]. Recent efforts to enhance activity of Re(I)-bipyridine and Mn(I)-bipyridine congeners have focused on modifying the secondary coordination sphere with Brønsted acidic substituents (e.g. hydroxyphenyl, imidazolium) [35-39]. This approach stabilizes the metallocarboxylate intermediate *via* intramolecular hydrogen bonding, resulting in a weakened C–O bond that rapidly dissociates water following protonation. A recent publication further extended the secondary coordination sphere concept in a Mn(I)-bipyridine to include methoxyphenyl Lewis bases which were capable of stabilizing the proposed metallocarboxylic acid intermediate that forms in the presence of weak Brønsted acids (e.g. 2,2,2-trifluoroethanol, phenol) [40]. While multiple ligand architectures deviating from substituted Re(I)-bipyridines have been recently reported to function as CO₂ reduction electrocatalysts [35, 41-46], surprisingly few reports exist describing Re(I)-phenanthroline analogues as catalysts [47-49].

Herein we report the synthesis, characterization, and electrocatalytic CO₂ reduction activity for a series of Re(I) catalysts of the design *fac*-[Re(R₂phen)(CO)₃Cl], where R₂phen is a 2,9-disubstituted-1,10-phenanthroline ligand (**Figure 1**). The substituents varied from possessing no steric bulk and minimal electronic contribution towards the Re(I) catalytic site (**Re(phen)**) to possessing steric hindrance and electron-donating substituents with possible weak hydrogen-bonding interactions (**Re((2,4,6-tmp)₂phen)**). In place of the more commonly used 2,2'-bipyridine architecture, substituted phenanthrolines were chosen given that the ligand's

backbone can be easily modified [50] to incorporate surface-anchoring substituents for heterogeneous catalysis [51-53]. Therefore, we sought to investigate the catalytic activity of the 1,10-phenanthroline architecture using various substituents at the 2 and 9 positions with the aim of future ligand expansion.

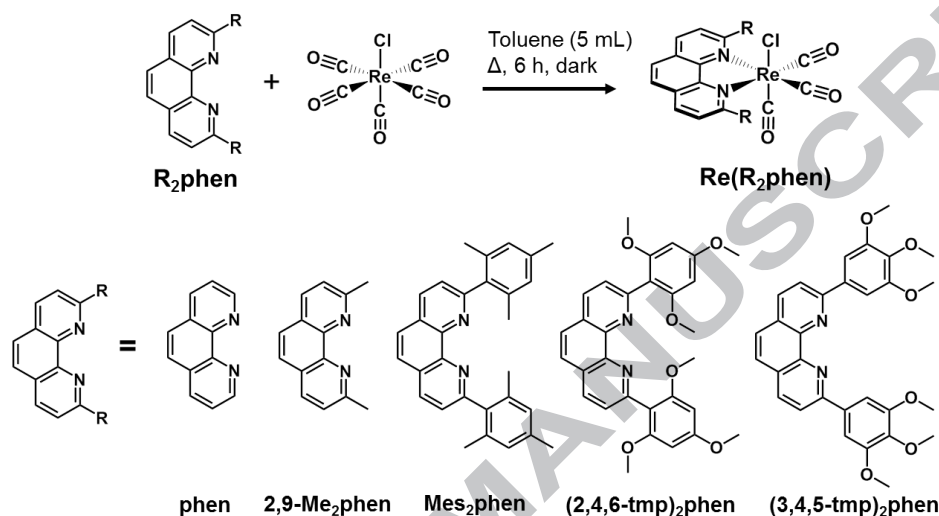


Figure 1. Structures of ligands and the corresponding synthesis of Re(I) electrocatalysts.

2. Experimental Details

2.1. Materials

All materials were used as received unless otherwise indicated. Pentacarbonylchlororhenium(I) (98%) and 2,4,6-trimethylphenylboronic acid (95%) were purchased from Acros Organics. 1,10-Phenanthroline (97%), 2,9-dichloro-1,10-phenanthroline (95+%), 2,4,6-trimethoxyphenylboronic acid (98%), and 3,4,5-trimethoxyphenylboronic acid (98%) were purchased from Ark Pharm. 2,9-Dimethyl-1,10-phenanthroline (98%) was purchased from Alfa Aesar. Tetrakis(triphenylphosphine)palladium(0) (98%) was purchased from Oakwood Chemical. Toluene, hexanes, CH_2Cl_2 , CH_3CN , and DMF solvents were purchased

from Fisher Scientific. It should be noted that the amount of H₂O reported to be present in CH₃CN and DMF solvents (0.003% and 0.02%, respectively) is a lower limit as the solvents were not extensively dried prior to analysis and atmospheric moisture may increase H₂O concentrations. Tetrabutylammonium hexafluorophosphate (98%), purchased from Alfa Aesar, was recrystallized using ethanol prior to electrochemical analyses and dried in a 110 °C oven. 2,9-Dimesityl-1,10-phenanthroline (**Mes₂phen**) [54], *fac*-[Re(phen)(CO)₃Cl] (**Re(phen)**), and *fac*-[Re(2,9-Me₂phen)(CO)₃Cl] (**Re(2,9-Me₂phen)**) [20, 52] were synthesized following previously established procedures.

2.2. Instrumentation

¹H and ¹³C NMR spectra were collected at 298 K using a Bruker Ascend spectrometer (500 MHz for ¹H and 125 MHz for ¹³C). Chemical shifts (ppm) were referenced to the residual solvent peak; CDCl₃ (¹H NMR) δ = 7.26 ppm, DMSO-*d*₆ (¹³C NMR) δ = 39.42 ppm [55]. High-resolution electrospray ionization mass spectrometry (HR-ESI-MS) was performed using a Thermo Fisher Scientific Q Exactive Plus hybrid quadrupole – Orbitrap mass spectrometer in positive mode. Samples were dissolved in HPLC-grade CH₃CN and a few drops of aqueous formic acid (0.1%) were added prior to injection. Elemental analysis (C, H, N combustion) was performed by Atlantic Microlabs, Inc. (Norcross, GA). Absorption spectra were recorded using an Agilent Cary 8454 diode array UV-visible spectrophotometer (1 nm resolution, 0.5 s integration time) in a 1 × 1 cm quartz cuvette (Starna Cells, Atascadero, CA) at room temperature. Molar absorptivity values were measured from gravimetrically prepared samples. IR spectra were collected in transmission mode using a Shimadzu IRAffinity-1S FT-IR spectrophotometer (average of 10 scans, 1 cm⁻¹ resolution), whereby samples were dissolved in CH₂Cl₂ solvent and added to a liquid IR cell equipped with CaF₂ windows.

2.3. Electrochemical measurements

Electrochemical measurements were performed using a BASi Epsilon EClipse™ electrochemical analyzer (Bioanalytical Systems Inc.; West Lafayette, Indiana, USA). Cyclic voltammograms (CV) were obtained using a standard three-electrode configuration with a glassy carbon (3 mm diameter) working electrode, a Pt wire auxiliary electrode, and a Ag/AgCl (3 M NaCl(aq)) reference electrode encapsulated in a glass tube with a Vycor® tip. Ferrocene (Fc) was added to the cell following each set of CV experiments, and potentials were referenced against the ferrocenium/ferrocene (Fc^+/Fc) couple (CH_3CN solvent: $E_{1/2}(\text{Fc}^+/\text{Fc}) = +0.45$ V vs. Ag/AgCl, $\Delta E_p = 90$ mV; DMF solvent: $E_{1/2}(\text{Fc}^+/\text{Fc}) = +0.56$ V vs. Ag/AgCl, $\Delta E_p = 120$ mV). Typical CVs were recorded with the following conditions: 0.5 mM complex in CH_3CN or DMF solvent, 0.1 M $n\text{-Bu}_4\text{NPF}_6$ supporting electrolyte, 200 mV/s scan rate, N_2 or CO_2 atmosphere, and 298 K temperature.

Controlled potential electrolysis (CPE) experiments were performed using a two-compartment H-cell separated by a fine porosity glass frit (Pine Research Instrumentation; Durham, North Carolina, USA). The auxiliary compartment consisted of a large surface area platinum disk auxiliary electrode that was submerged in a 25 mL, N_2 - or CO_2 -saturated electrolyte solution (0.1 M $n\text{-Bu}_4\text{NPF}_6$). The working compartment contained a 45 ppi (pore per linear inch) vitreous reticulated carbon working electrode and a Ag/AgCl (3 M NaCl(aq)) reference electrode encapsulated in a glass tube with a Vycor® tip, both of which were submerged in a 25 mL, N_2 - or CO_2 -saturated electrolyte solution (0.1 M $n\text{-Bu}_4\text{NPF}_6$) containing 0.5 mM Re(I)-diimine catalyst. The working compartment was rapidly stirred to ensure efficient mass transport throughout the solution. After 1 h electrolysis at -2.75 V vs. Fc^+/Fc , a 100 μL aliquot of the working compartment's headspace was sampled using a Hamilton sample lock

GASTIGHT[®] syringe and injected into a Shimadzu GC-2014 gas chromatograph (ultra high purity He carrier gas) with a packed ShinCarbon ST SilicoSmooth stainless steel column (2 m long × 1/8 in. o.d. × 2.0 mm i.d.; 80/100 mesh) and a Shimadzu TCD-2014 thermal conductivity detector. The GC conditions were as follows: injector temp, 200 °C; column temperature, 64 °C; detector temperature, 200 °C; detector current, 120 mA; and gas flow, 20 mL/min. The evolution of CO from the CPE experiments was confirmed by comparing the retention times with a CO gas standard.

2.4. Synthesis of 2,9-Bis-(2,4,6-trimethoxyphenyl)-1,10-phenanthroline ((2,4,6-tmp)₂phen)

Ligand **(2,4,6-tmp)₂phen** was prepared following synthetic procedures for the dimesityl-substituted analogue (**Mes₂phen**) [54]. In a round bottom flask, 2,9-dichloro-1,10-phenanthroline (0.225 g, 0.903 mmol) and 2,4,6-trimethoxyphenylboronic acid (0.440 g, 2.08 mmol) were suspended in 18.4 mL of toluene and 7.9 mL of 2 M Na₂CO₃(aq), then purged with argon for 15 min. A catalytic amount of Pd(PPh₃)₄ (0.1 eq, 0.104 g, 0.090 mmol) was added and the reaction mixture was heated at reflux for 48 hours. The biphasic reaction mixture was cooled to room temperature, and the organic layer was separated from the aqueous layer and set aside. The aqueous layer was washed with dichloromethane and the organic fractions were combined, dried using anhydrous MgSO₄, and filtered. The solvent was removed *via* rotary evaporation and the remaining solid was suspended in cold diethyl ether and filtered. Yield = 0.336 g (0.656 mmol, 72.6%). ¹H NMR (500 MHz, 298 K, CDCl₃): δ (ppm) = 8.20 (d, 2H, *J* = 7.9 Hz; 4, 7), 7.78 (s, 2H; 5, 6), 7.61 (d, 2H, *J* = 8.2 Hz; 3, 8), 6.23 (s, 4H; *meta*), 3.85 (s, 6H; *para* OCH₃), 3.73 (s, 12H; *ortho* OCH₃). ¹³C NMR (125 MHz, 298 K, DMSO-*d*₆): δ (ppm) = 161.09, 158.40, 154.78, 145.42, 135.63, 127.03, 126.13, 126.10, 112.43, 91.07, 55.65, 55.42. HR-ESI(+)-MS: [M + H]⁺

$m/z = 513.2022$ (calc. $m/z = 513.2020$). Elemental analysis calculated for $C_{30}H_{28}N_2O_6$: 70.29% C, 5.52% H, 5.47% N. Found: 69.53% C, 5.45% H, 5.54% N.

2.5. Synthesis of 2,9-Bis-(3,4,5-trimethoxyphenyl)-1,10-phenanthroline ((3,4,5-tmp)₂phen)

Ligand **(3,4,5-tmp)₂phen** was prepared using the same procedure as described for **(2,4,6-tmp)₂phen**, except 2,9-dichloro-1,10-phenanthroline (0.350 g, 1.40 mmol) and 3,4,5-trimethoxyphenylboronic acid (0.750 g, 3.50 mmol) were used. Yield = 0.467 g (0.911 mmol, 65%). ¹H NMR (500 MHz, 298 K, CDCl₃): δ (ppm) = 8.31 (d, 2H, $J = 8.2$ Hz; 4, 7), 8.09 (d, 2H, $J = 8.2$ Hz; 3, 8), 7.80 (s, 2H; 5, 6), 7.70 (s, 4H; *ortho*), 4.05 (s, 12H; *meta* OCH₃), 3.96 (s, 6H; *para* OCH₃). ¹³C NMR (125 MHz, 298 K, DMSO-*d*₆): δ (ppm) = 154.98, 153.39, 145.14, 139.77, 137.25, 134.51, 127.77, 126.09, 120.12, 105.77, 60.27, 56.52. HR-ESI(+)-MS: $[M + H]^+$ $m/z = 513.2021$ (calc. $m/z = 513.2020$). Elemental analysis calculated for $C_{30}H_{28}N_2O_6 \cdot H_2O$: 67.98% C, 5.66% H, 5.28% N. Found: 67.85% C, 5.75% H, 5.23% N.

2.6. Synthesis of *fac*-[Re(*Mes*₂phen)(CO)₃Cl] (*Re*(*Mes*₂phen))

An aliquot of Re(CO)₅Cl (0.0493 g, 0.138 mmol) and **Mes₂phen** ligand (0.0579 g, 0.139 mmol) were added to a 25 mL round bottom Schlenk flask equipped with a magnetic stir bar. Toluene (5 mL) was added and the mixture was deoxygenated for 10 min using Ar while at room temperature. The mixture was then heated at reflux for 6 h in the dark while under a blanket of Ar. After 15 min, the white mixture changed to yellow and eventually yellow solids began to precipitate from the reaction. After 6 h, the resulting yellow mixture was cooled to room temperature and the yellow solids were collected by vacuum filtration, followed by rinsing with hexanes. Yield = 0.0595 g (0.0824 mmol, 60%). ¹H NMR (500 MHz, 298 K, CDCl₃): δ (ppm) = 8.52 (d, 2H, $J = 8.2$ Hz; 4, 7), 8.05 (s, 2H; 5, 6), 7.71 (d, 2H, $J = 8.2$ Hz; 3, 8), 7.03 (s, 4H; *meta*), 2.38 (s, 6H; CH₃), 2.20 (s, 6H; CH₃), 2.00 (s, 6H; CH₃). ¹³C NMR (125 MHz, 298 K, DMSO-*d*₆):

δ (ppm) = 192.15, 163.86, 147.33, 140.00, 138.96, 135.47, 134.86, 129.79, 128.49, 128.08, 127.64, 127.25, 20.83, 20.75, 19.79. FTIR (CH₂Cl₂) ν (CO): 2024 cm⁻¹, 1925 cm⁻¹, 1889 cm⁻¹. HR-ESI(+)-MS: [M + Na]⁺ m/z = 745.1243 (calc. m/z = 745.1244), [M] m/z = 722.1348 (calc. m/z = 722.1341), [M - Cl]⁺ m/z = 687.1665 (calc. m/z = 687.1658). Elemental analysis calculated for C₃₃H₂₈N₂O₃ClRe·H₂O: 53.56% C, 4.05% H, 3.78% N. Found: 53.49% C, 3.97% H, 3.86% N.

2.7. Synthesis of *fac*-[Re((2,4,6-*tmp*)₂phen)(CO)₃Cl] (**Re((2,4,6-*tmp*)₂phen)**)

The target complex was prepared using the same procedure as described above, except Re(CO)₅Cl (0.0141 g, 0.0340 mmol) and **(2,4,6-*tmp*)₂phen** ligand (0.0202 g, 0.0394 mmol) were used. Yield = 0.0227 g (0.0277 mmol, 81%). ¹H NMR (500 MHz, 298 K, CDCl₃): δ (ppm) = 8.41 (d, 2H, *J* = 8.2 Hz; 4, 7), 7.94 (s, 2H; 5, 6), 7.73 (d, 2H, *J* = 8.2 Hz; 3, 8), 6.29 (d, 2H, *J* = 2.0 Hz; *meta*), 6.24 (d, 2H, *J* = 2.0 Hz; *meta*), 3.89 (s, 6H; OCH₃), 3.79 (s, 6H; OCH₃), 3.66 (s, 6H; OCH₃). ¹³C NMR (125 MHz, 298 K, DMSO-*d*₆): δ (ppm) = 194.31, 162.94, 159.08, 158.58, 158.15, 147.41, 138.36, 129.16, 128.48, 126.94, 112.75, 91.61, 90.63, 56.19, 55.53, 55.26. FTIR (CH₂Cl₂) ν (CO): 2018 cm⁻¹, 1913 cm⁻¹, 1890 cm⁻¹. HR-ESI(+)-MS: [M - Cl]⁺ m/z = 783.1340 (calc. m/z = 783.1347). Elemental analysis calculated for C₃₃H₂₈N₂O₉ClRe: 48.43% C, 3.46% H, 3.42% N. Found: 48.46% C, 3.74% H, 3.30% N.

2.8. Synthesis of *fac*-[Re((3,4,5-*tmp*)₂phen)(CO)₃Cl] (**Re((3,4,5-*tmp*)₂phen)**)

The target complex was prepared using the same procedure as described above, except Re(CO)₅Cl (0.0495 g, 0.138 mmol) and **(3,4,5-*tmp*)₂phen** ligand (0.0706 g, 0.138 mmol) were used. Yield = 0.0986 g (0.120 mmol, 87%). ¹H NMR (500 MHz, 298 K, CDCl₃): δ (ppm) = 8.55 (d, 2H, *J* = 8.2 Hz; 4, 7), 8.06 (s, 2H; 5, 6), 7.95 (d, 2H, *J* = 8.2 Hz; 3, 8), 6.99 (s, 2H; *ortho*), 6.87 (s, 2H; *ortho*), 3.95 (s, 6H; OCH₃), 3.94 (s, 6H; OCH₃), 3.90 (s, 6H; OCH₃). ¹³C NMR (125

MHz, 298 K, DMSO-*d*₆): δ (ppm) = 193.60, 163.38, 153.03, 152.69, 147.03, 139.35, 139.29, 137.20, 129.87, 127.36, 127.08, 107.75, 60.15, 56.32, 55.90. FTIR (CH₂Cl₂) ν (CO): 2022 cm⁻¹, 1924 cm⁻¹, 1884 cm⁻¹. HR-ESI(+)-MS: [M - Cl]⁺ m/z = 783.1344 (calc. m/z = 783.1347). Elemental analysis calculated for C₃₃H₂₈N₂O₉ClRe: 48.43% C, 3.46% H, 3.42% N. Found: 48.15% C, 3.53% H, 3.47% N.

3. Results and Discussion

The Re(I) phenanthroline electrocatalysts were originally designed to provide varied steric bulk, electronic contribution, and potential weak hydrogen bonding sites towards the Re metal center with the aim of evaluating their respective effects on electrocatalytic CO₂ reduction. Compared to the unsubstituted 1,10-phenanthroline (**phen**), inclusion of methyl (**2,9-Me₂phen**) and trimethylphenyl (**Mes₂phen**) substituents at the 2 and 9 positions introduces steric bulk near the metal center. These added substituents also enhance the electron density on the phenanthroline ligand, inducing a small cathodic shift in the reduction potentials of both the R₂phen^{0/-} and Re^{I/0} redox couples (*vide infra*). Trimethoxyphenyl (**(2,4,6-tmp)₂phen** and **(3,4,5-tmp)₂phen**) substituents were selected to not only provide steric bulk and an electronic contribution, but also to introduce Lewis basic sites capable of weak hydrogen bonding to stabilize the proposed metallocarboxylic acid intermediate (Re-CO₂H). However, this work showed that the electronic effects dominate the observed catalytic activity.

3.1. Synthesis and characterization

The new trimethoxyphenyl-substituted phenanthroline ligands were synthesized in good yield using well-established Suzuki-Miyaura cross-coupling reaction conditions [54, 56]. ¹H and ¹³C NMR spectra of **(2,4,6-tmp)₂phen** and **(3,4,5-tmp)₂phen** (Supporting Information, **Figures S1 – S4**) agree well with the expected splitting patterns and chemical shifts for the symmetric

(C_{2v}), trimethoxyphenyl-substituted architecture. High-resolution ESI-MS (**Figures S5 and S6**) and elemental analysis further corroborate the proposed molecular weight and C, H, N elemental composition, respectively.

The *fac*-[Re(R_2 phen)(CO)₃Cl] complexes were prepared by combining the substituted-phenanthroline ligands with Re(CO)₅Cl (1:1 ratio) in toluene and heating at reflux (Ar atm, dark, 6 h) to afford bright yellow solids. ¹H NMR spectra for the new **Re(Mes₂phen)**, **Re((2,4,6-tmp)₂phen)**, and **Re((3,4,5-tmp)₂phen)** complexes (see Supporting Information) show three proton resonance signals ranging from $\delta = 7.6 - 8.6$ ppm (two doublets and one singlet in each spectrum), consistent with a symmetrically-substituted phenanthroline backbone coordinated to the Re^I(CO)₃Cl core. Furthermore, the **Re((2,4,6-tmp)₂phen)** and **Re((3,4,5-tmp)₂phen)** trimethoxyphenyl-substituted structures display the expected downfield OCH₃ singlets ($\delta = 3.65 - 3.95$ ppm) compared to the trimethylphenyl-substituted **Re(Mes₂phen)** CH₃ singlets located upfield ($\delta = 2.00 - 2.40$ ppm). Three OCH₃ and CH₃ signals are observed for the trimethoxyphenyl and trimethylphenyl complexes, respectively, which further attest to their symmetric architecture. More specifically, the three carbonyl substituents are in a *facial* arrangement around the Re metal center with C_s symmetry (one mirror plane bisecting the phenanthroline ligand).

FTIR spectra for all Re(I) complexes (**Figure S16**) were obtained in CH₂Cl₂ solvent and agree well with a *fac*-[Re(R_2 phen)(CO)₃Cl] geometry of C_s symmetry whereby three carbonyl stretching vibrations (order of energy: $A'(1) > A'(2) > A''$) are observed in the range of $\nu(\text{CO}) = 2024 - 1884 \text{ cm}^{-1}$ [57]. As shown in **Table 1**, the new **Re(Mes₂phen)**, **Re((2,4,6-tmp)₂phen)**, and **Re((3,4,5-tmp)₂phen)** complexes possess features in agreement with the structurally-similar *fac*-[Re(dap)(CO)₃Cl] (dap = 2,9-di-anisyl-1,10-phenanthroline), which displays three CO

stretching vibrations at $\nu(\text{CO}) = 2022, 1924, \text{ and } 1884 \text{ cm}^{-1}$ when measured in CH_2Cl_2 solvent [58]. Of note is the shift to lower energy of the $A'(1)$ symmetric vibration in **Re((2,4,6-tmp)₂phen)** ($\nu(\text{CO}) = 2018 \text{ cm}^{-1}$). This shift is indicative of increased electron density at the Re(I) center, resulting from enhanced π -backbonding between the $\text{Re}(d\pi)$ and $\text{CO}(\pi^*)$ molecular orbitals, thus weakening the C–O vibration. As described below, methoxy substituents at the *ortho* and *para* positions of the phenyl ring contribute electron density into the phenanthroline ligand, and ultimately to the Re metal center.

Table 1. Carbonyl vibrational frequencies $\nu(\text{CO})$ for *fac*-[Re(R₂phen)(CO)₃Cl] complexes ^a

Complex	A'(1)	A'(2)	A''
Re(phen)	2024	1921	1898
Re(2,9-Me ₂ phen)	2024	1916	1896
Re(Mes ₂ phen)	2024	1925	1889
Re((2,4,6-tmp) ₂ phen)	2018	1913	1890
Re((3,4,5-tmp) ₂ phen)	2022	1924	1884
<i>fac</i> -[Re(dap)(CO) ₃ Cl] ^b	2022	1924	1884

^a Measured in CH_2Cl_2 solvent; values reported as cm^{-1} . ^b Reference [58].

The new trimethylphenyl and trimethoxyphenyl complexes possess UV and visible light absorbing properties similar to previously reported Re(I)-diimine carbonyl complexes [59-61]. As illustrated in **Figure 2**, the UV region is dominated by intense R₂phen-based intraligand (¹IL) $\pi \rightarrow \pi^*$ transitions ($\lambda_{\text{abs}} \sim 264 \text{ nm}$), whereby the inclusion of substituted aryl groups at the 2 and 9 positions on 1,10-phenanthroline extend the UV light absorbing character past 350 nm. The broad, featureless transition extending into the visible region is assigned to the $\text{Re}(d\pi) \rightarrow \text{R}_2\text{phen}(\pi^*)$ metal-to-ligand charge transfer (¹MLCT) transition for each complex. The

methyl-substituted **Re(2,9-Me₂phen)** (not shown to minimize overcrowding) absorbs at $\lambda_{\text{abs}} = 370$ nm, in agreement with a previously reported value [60]. **Re(Mes₂phen)** ($\lambda_{\text{abs}} = 375$ nm; $\epsilon = 3,140 \text{ M}^{-1}\text{cm}^{-1}$) displays similar absorption characteristics as **Re(phen)** ($\lambda_{\text{abs}} = 370$ nm; $\epsilon = 3,900 \text{ M}^{-1}\text{cm}^{-1}$), indicating that trimethylphenyl substituents do not strongly modify the electronic structure within this architecture. Similarly, the ¹MLCT for the trimethoxyphenyl analogues tails into the visible region and is somewhat overshadowed by the encroaching R₂phen $\pi \rightarrow \pi^*$ transitions, making it difficult to assign a $\lambda_{\text{abs}}^{\text{max}}$ value. However, based on electrochemical data (*vide infra*) and analogous complexes, the lowest energy absorption for **Re((2,4,6-tmp)₂phen)** and **Re((3,4,5-tmp)₂phen)** is also ¹MLCT in nature.

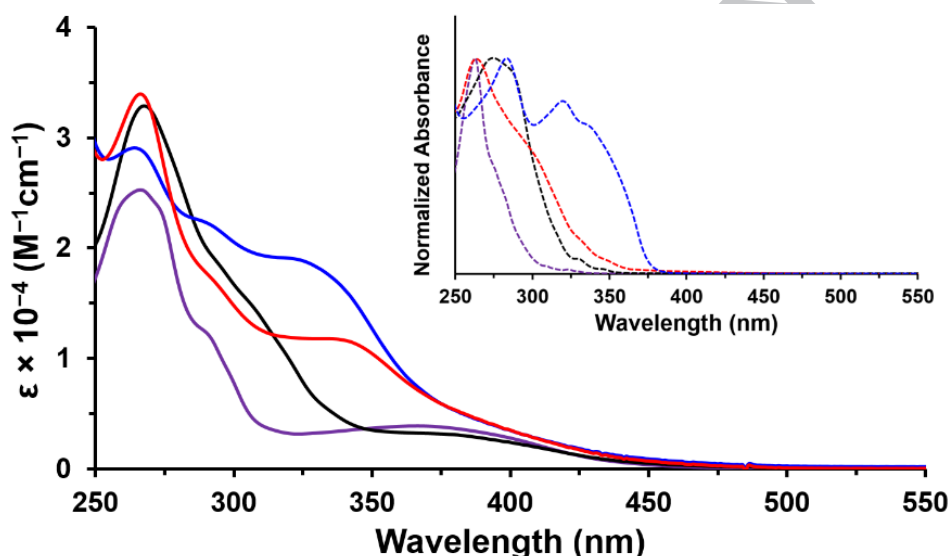


Figure 2. Electronic absorption spectra of complexes **Re(phen)** (—), **Re(Mes₂phen)** (—), **Re((2,4,6-tmp)₂phen)** (—), and **Re((3,4,5-tmp)₂phen)** (—) in CH₃CN. Inset displays the normalized absorption profile for the corresponding free ligands (**phen** (---), **Mes₂phen** (---), **(2,4,6-tmp)₂phen** (---), and **(3,4,5-tmp)₂phen** (---)) over the same range of wavelengths.

3.2. Electrochemical properties under N_2 atmosphere

Electrochemical properties of the new trimethylphenyl- and trimethoxyphenyl-substituted complexes were first analyzed under an inert atmosphere (N_2) to better understand how sterics and electronics affect the redox characteristics. CVs of all Re(I) complexes were recorded in N_2 -saturated CH_3CN and DMF solvents (**Figures 3** and **4**, respectively), and a summary of the pertinent redox potentials is listed in **Table 2**. As expected, the complexes display a Re-based HOMO and diimine-based LUMO, with similar redox characteristics to those for structurally-related *fac*-[Re(NN)(CO)₃Cl] complexes (NN = substituted 2,2'-bipyridine or 1,10-phenanthroline ligand) [62, 63].

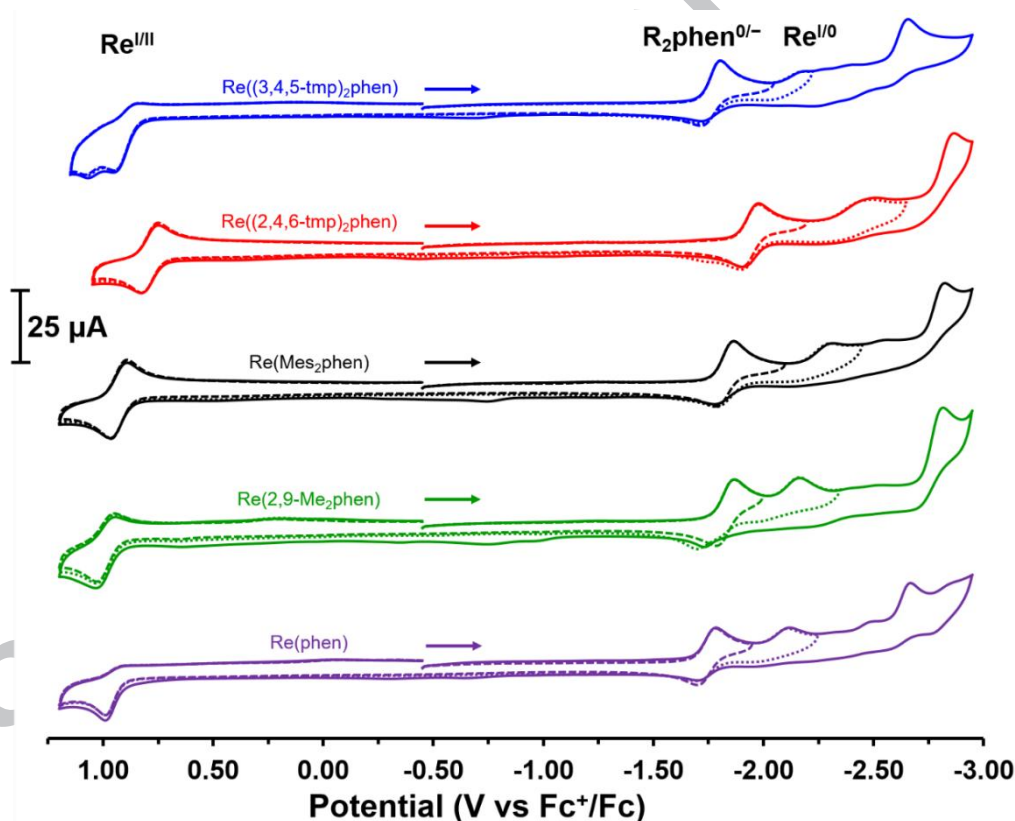


Figure 3. Cyclic voltammograms of **Re(phen)** (purple lines), **Re(2,9-Me₂phen)** (green lines), **Re(Mes₂phen)** (black lines), **Re((2,4,6-tmp)₂phen)** (red lines), and **Re((3,4,5-tmp)₂phen)** (blue lines) measured in CH_3CN solvent under a N_2 atmosphere. Conditions: 0.5 mM Re(I) complex, 0.1 M *n*-Bu₄NPF₆ electrolyte, 200 mV/s scan rate, RT. The arrow indicates the scan direction.

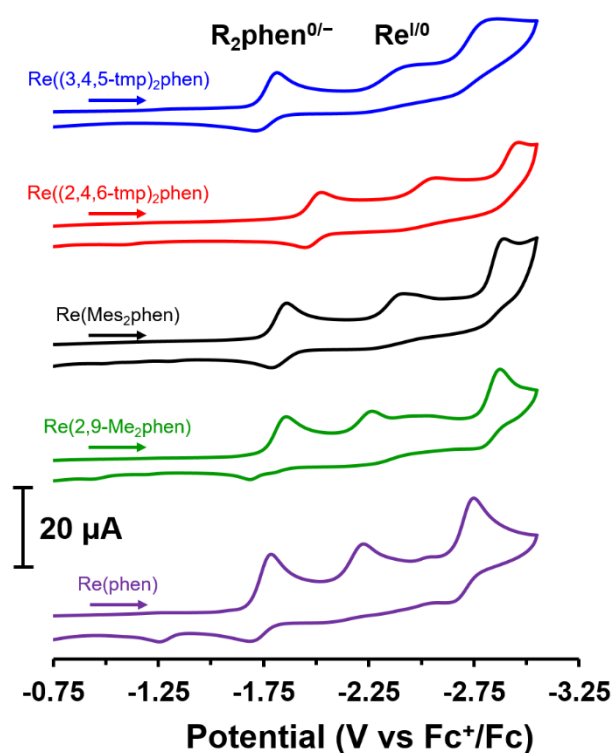


Figure 4. Cathodic cyclic voltammograms of **Re(phen)** (purple lines), **Re(2,9-Me₂phen)** (green lines), **Re(Mes₂phen)** (black lines), **Re((2,4,6-tmp)₂phen)** (red lines), and **Re((3,4,5-tmp)₂phen)** (blue lines) measured in DMF solvent under a N₂ atmosphere. Conditions: 0.5 mM Re(I) complex, 0.1 M *n*-Bu₄NPF₆ electrolyte, 200 mV/s scan rate, RT. The arrow indicates the scan direction.

Anodic CVs collected in CH₃CN (**Figure 3**) illustrate how ligand substitution modifies the Re^{III} chemical reversibility and oxidation potential. At $v = 200$ mV/s, the unsubstituted **Re(phen)** displays a chemically irreversible Re^{III} oxidation at $E_p^a = +0.99$ V vs. Fc⁺/Fc. This is attributed to the rapid dimerization of two [Re^{II}(phen)(CO)₃Cl]⁺ species via a chloride bridge, which undergoes disproportionation and attack by a solvent molecule forming [Re^I(phen)(CO)₃(CH₃CN)]⁺ and [Re^{III}(phen)(CO)₃Cl₂]⁺ [63]. Methyl substituents in **Re(2,9-Me₂phen)** introduce enough steric bulk to increase the chemical reversibility of the Re^{III} couple by inhibiting the rapid coordination of a solvent molecule. Further increasing the steric bulk with

Re(Mes₂phen) and **Re((2,4,6-tmp)₂phen)** produces a chemically reversible $\text{Re}^{\text{I/II}}$ couple at $E_{1/2} = +0.93$ and $+0.79$ V, respectively, in line with the steric contribution inhibiting solvent coordination [63]. Furthermore, the presence of methyl and methoxy substituents at the *ortho* and *para* positions of the phenyl ring adds electron density into the phenanthroline ligand, destabilizing the $\text{Re}(\text{d}\pi)$ -based HOMO as evident by the less positive $E_{1/2}(\text{Re}^{\text{I/II}})$. The 3,4,5-trimethoxyphenyl-substituted complex, **Re((3,4,5-tmp)₂phen)**, displays a quasi-reversible couple at $E_{1/2} = +0.89$ V, followed by an irreversible wave at $E_p^a = +1.07$ V, the latter of which may involve irreversible oxidation of the *meta*-positioned methoxy groups on the phenyl ring [64]. The change in reversibility and the shift to a more positive potential compared to the 2,4,6-substituted analogue emphasizes the profound steric and electronic impact of *ortho* vs. *meta* positions on the phenyl ring. The *meta*-positioned methoxy groups withdraw electron density from the ring system, while also providing smaller steric bulk than the *ortho* methyl and methoxy substituents in **Re(Mes₂phen)** and **Re((2,4,6-tmp)₂phen)**, respectively.

In both CH_3CN and DMF solvents, cathodic scans reveal the rich and complex electrochemistry also observed for previously reported $\text{Re}(\text{I})$ complexes [4, 20, 62]. This discussion will refer primarily to the properties observed in CH_3CN , but similar trends are observed in DMF solvent. The first redox couple is assigned to the quasi-reversible $\text{R}_2\text{phen}^{0/-}$ reduction. Subsequent processes involve competing mechanisms that undergo Cl^- dissociation and $\text{Re}^{\text{I/0}}$ reduction (ECE mechanism; E = electron transfer, C = chemical step) or an irreversible $\text{Re}^{\text{I/0}}$ reduction and rapid Cl^- dissociation (EEC mechanism). Electron donor effects from the methyl (**Re(2,9-Me₂phen)**) and trimethylphenyl (**Re(Mes₂phen)**) substituents cathodically shift the $\text{R}_2\text{phen}^{0/-}$ reduction ($E_{1/2}(\text{R}_2\text{phen}^{0/-}) = -1.83$ and -1.82 V, respectively) compared to the unsubstituted analogue **Re(phen)** ($E_{1/2}(\text{R}_2\text{phen}^{0/-}) = -1.74$ V). Interestingly, the methyl and

trimethylphenyl substituents influence the electronics within the phenanthroline π -system to a similar degree as evidenced by the nearly identical $\text{Re}_2\text{phen}^{0/-}$ potential; however, the trimethylphenyl exhibits a more negative shift in the $\text{Re}^{\text{I}0}$ reduction, suggesting the latter contributes more strongly to the σ -donating component (i.e. inductive effects).

Introduction of methoxy Lewis basic groups in the *ortho* and *para* positions in **Re((2,4,6-tmp)₂phen)** display more negative reduction potentials ($E_{1/2}(\text{Re}_2\text{phen}^{0/-}) = -1.94$ V; $E_p^c(\text{Re}^{\text{I}0}) = -2.49$ V) than **Re(Mes₂phen)**, indicating the increased electron donating character as a result of the methoxy substituents. In contrast, the presence of methoxy groups at the *meta* position in **Re((3,4,5-tmp)₂phen)** lead to less negative reduction potentials ($E_{1/2}(\text{Re}_2\text{phen}^{0/-}) = -1.76$ V; $E_p^c(\text{Re}^{\text{I}0}) = -2.17$ V) that are comparable to **Re(phen)**, which further confirms the electron withdrawing character of *meta*-substituted methoxy substituents. The steric crowding and electronic push-pull effect are expected to contribute to the observed electrocatalytic CO_2 reduction within this substituted-phenanthroline architecture.

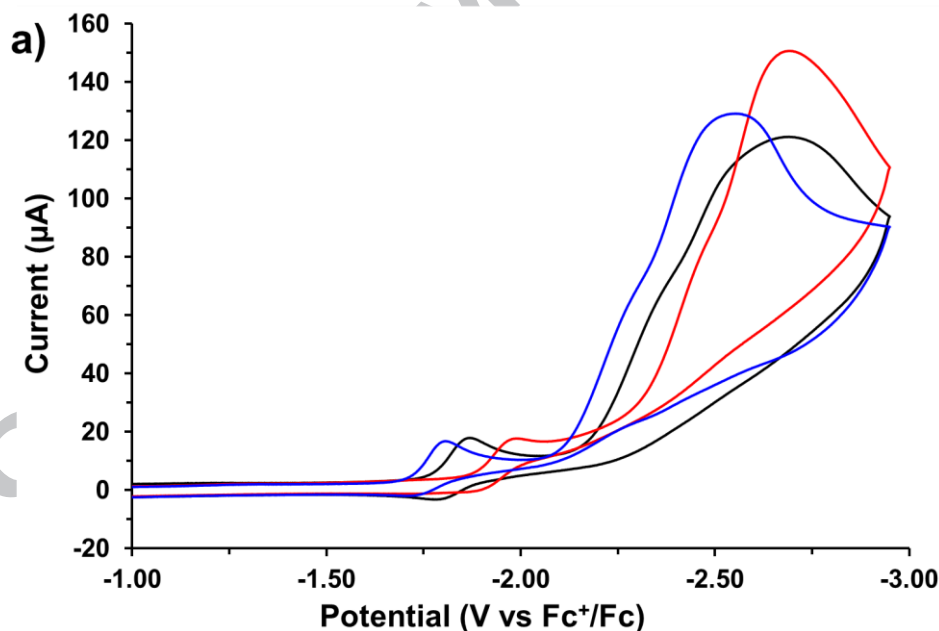
Table 2. Redox properties of Re(I) electrocatalysts in CH_3CN and DMF solvents ^a

Complex	$E_{1/2}(\text{Re}^{\text{II}}) / \text{V}$	$E_{1/2}(\text{Re}_2\text{phen}^{0/-}) / \text{V}$		$E_p^c(\text{Re}^{\text{I}0}) / \text{V}^b$	
	CH_3CN	CH_3CN	DMF	CH_3CN	DMF
Re(phen)	+0.99 ^c	-1.74	-1.75	-2.11	-2.23
Re(2,9-Me ₂ phen)	+0.99	-1.83	-1.83	-2.16	-2.28
Re(Mes ₂ phen)	+0.93	-1.82	-1.83	-2.30	-2.43
Re((2,4,6-tmp) ₂ phen)	+0.79	-1.94	-1.99	-2.49	-2.58
Re((3,4,5-tmp) ₂ phen)	+0.89 ^d	-1.76	-1.77	-2.17	-2.48

^a Reported $E_{1/2}$ values were measured using 0.5 mM Re(I) catalyst, 0.1 M *n*-Bu₄NPF₆ electrolyte, RT, N₂ atm, and 200 mV/s scan rate. Potentials referenced against the Fc⁺/Fc reversible redox couple. ^b Reported E_p^c for an irreversible reductive process. ^c Reported E_p^a for an irreversible oxidative process. ^d Reported $E_{1/2}$ for a quasi-reversible oxidative process.

3.3. Electrocatalytic activity under CO₂ atmosphere

The electrocatalytic activity for all five *fac*-[Re(R₂phen)(CO)₃Cl] complexes was determined by CV analysis in both CO₂-saturated CH₃CN and DMF solvents. The results are shown in **Figure 5** for complexes **Re(Mes₂phen)**, **Re((3,4,5-tmp)₂phen)**, and **Re((2,4,6-tmp)₂phen)**, and all additional CVs are provided in the Supporting Information (**Figures S17 – S27**). For all complexes, an increase in cathodic current is observed at the Re^{I/0} redox wave and is characteristic of catalytic CO₂ reduction, indicating that the two-electron reduced Re-phenanthroline species, [Re⁰(R₂phen⁻)(CO)₃]⁻, is the dominant mechanism to enable rapid catalytic turnover. To confirm the formation of CO gas, controlled potential electrolysis (CPE) was performed by applying -2.75 V vs Fc⁺/Fc under a CO₂-saturated atmosphere and sampling the headspace above the electrolysis solution.



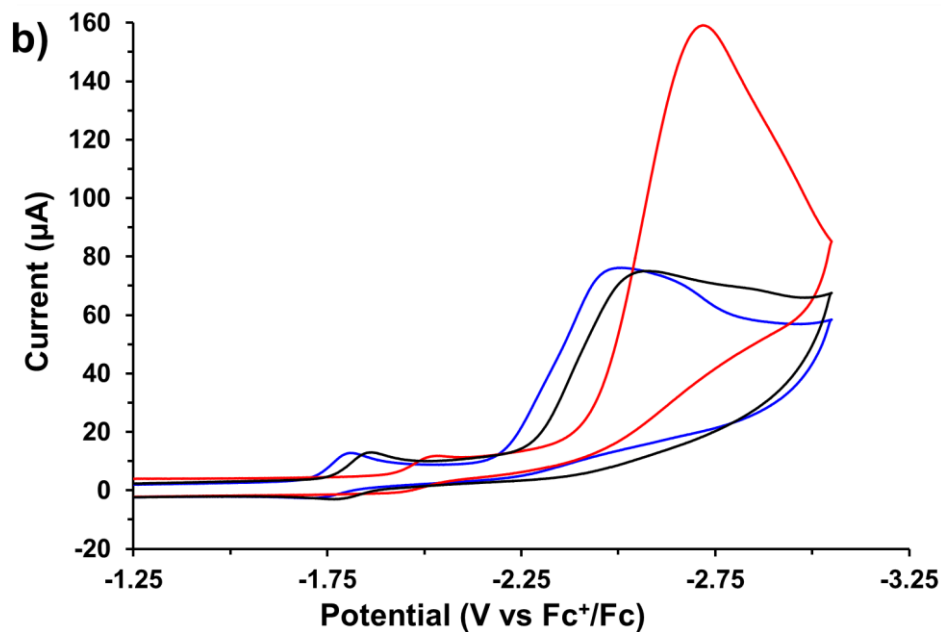


Figure 5. Cyclic voltammograms measured under CO₂ atm in CH₃CN (a) and DMF (b). CVs of **Re(Mes₂phen)** (black), **Re((2,4,6-tmp)₂phen)** (red), and **Re((3,4,5-tmp)₂phen)** (blue) using 0.5 mM Re(I) catalyst, 0.1 M *n*-Bu₄NPF₆ electrolyte, 200 mV/s scan rate, RT.

In order to compare the electrocatalytic CO₂ reduction activity between each complex, the current response ratio (i_{cat}/i_p) was determined from the current for a non-catalytic one-electron reduction under N₂ (i_p) and the catalytic current under CO₂ (i_{cat}) [65]. The calculated i_{cat}/i_p values are tabulated in **Table 3** for each complex in CH₃CN and DMF. The methyl-substituted **Re(2,9-Me₂phen)** exhibits a small increase of catalytic activity compared to **Re(phen)**, indicating the methyl substituent's minimal electronic and steric effects. The sterically bulky, electron donating trimethylphenyl groups in **Re(Mes₂phen)** further enhance CO₂ reduction activity, likely the result of the more negative Re^{I/0} reduction displayed in the redox characteristics under N₂. In both CH₃CN and DMF solvents, a small increase in activity occurs when methoxy groups are introduced at the *meta* and *para* positions in **Re((3,4,5-tmp)₂phen)**, accompanied by a small shift to less negative potential for the catalytic wave. By changing the position of the methoxy

groups from *meta* to *ortho*, **Re((2,4,6-tmp)₂phen)** displays an additional increase in the i_{cat}/i_p ratio compared to **Re((3,4,5-tmp)₂phen)** when analyzed in either DMF or CH₃CN. This indicates that the strong electron donating effects of *ortho/para* vs. *meta/para*-substituted methoxy groups, evidenced by the redox properties under N₂, play a significant role in the catalytic enhancement.

Table 3. Electrocatalytic activity of Re(I) catalysts ^a

Complex	DMF	CH ₃ CN
	i_{cat}/i_p	i_{cat}/i_p
Re(phen)	4.1	4.2
Re(2,9-Me ₂ phen)	4.9	4.6
Re(Mes ₂ phen)	5.4	6.8
Re((2,4,6-tmp) ₂ phen)	14.8	8.5
Re((3,4,5-tmp) ₂ phen)	6.0	7.7

^a Values were determined from CVs collected using 0.5 mM Re(I) catalyst, 0.1 M *n*-Bu₄NPF₆ in DMF or CH₃CN electrolyte system, room temperature, CO₂ atm, and 200 mV/s scan rate. i_{cat}/i_p values were determined from the ratio of the peak catalytic current response under CO₂ atmosphere (i_{cat}) and the current response for a non-catalytic one-electron reduction under N₂ atmosphere (i_p).

3.4. Solvent contribution to catalytic activity

During the electrocatalytic analyses under CO₂ atmosphere, we observed varying degrees of catalytic enhancement in CH₃CN and DMF solvents depending on which Re catalyst was used, and therefore must comment on this phenomenon. A comparison of the catalytic activity in DMF and CH₃CN for each Re catalyst is provided in **Table 3**. Note that the absolute value of the currents and i_{cat}/i_p ratios between solvents should be compared with caution due to differences in

solvent properties such as CO₂ solubility and diffusion rates. However, the trend in current enhancement ratios (i_{cat}/i_p) within a solvent series provides useful insight into the solvent's role in electrocatalysis. A 2.5x increase in the i_{cat}/i_p ratio is observed for **Re((2,4,6-tmp)₂phen)** compared to **Re((3,4,5-tmp)₂phen)** in DMF ($i_{cat}/i_p = 14.8$ vs. 6.0, respectively), but only a small increase is observed in CH₃CN ($i_{cat}/i_p = 8.5$ vs. 7.7, respectively). This significant difference in activity based on the solvent used and the proximity of the methoxy substituents to the Re active site highlights how the electrocatalysts' design and solvent system should be carefully considered.

A recent publication reporting *fac*-[Re(pyridine-oxazoline)(CO)₃Cl] complexes as CO₂ reduction electrocatalysts showed how the Lewis basicity of the solvent (i.e. the donor number, DN) greatly affects the rate of catalysis, whereby the calculated rate constant for CO₂ reduction decreased as the solvent's DN increased [42]. It was suggested that stronger Lewis basic solvents such as DMF and DMSO (DN = 26.6 and 29.8, respectively) more effectively hydrogen bond with the metallocarboxylic acid intermediate than CH₃CN (DN = 14.1) and/or compete more strongly for available protons, which serve to protonate the metallocarboxylate intermediate. Both processes are expected to suppress rapid CO₂ reduction activity and the study emphasizes how the Lewis basicity of a solvent can dominate the observed reactivity. Within our study, only **Re((2,4,6-tmp)₂phen)** displayed a significant current enhancement using the stronger Lewis basic solvent DMF compared to the weaker Lewis basic solvent CH₃CN. We originally considered weak intramolecular hydrogen bonding between the proximal methoxy substituents and a metallocarboxylic acid intermediate (Re-CO₂H) being capable of suppressing the strong Lewis basicity of DMF as a solvent for electrocatalysis. Hydrogen-bonding intermediates typically lower the energetic barrier for CO₂ reduction and result in an anodic shift of the

catalytic wave; however, our CVs in DMF still display relatively cathodic potentials for catalysis. The significant activity increase in DMF for **Re((2,4,6-tmp)₂phen)** compared to **Re(Mes₂phen)** and **Re((3,4,5-tmp)₂phen)** does suggest a solvent-mediated pathway which couples the electronic and Lewis basic character of the proximal methoxy substituents with the solvent. However, the exact mechanism by which the solvent influences catalysis requires further investigation and these results warrant such analysis.

4. Conclusions

We have synthesized and characterized a new series of *fac*-[Re(R₂phen)(CO)₃Cl] complexes containing varying degrees of steric bulk and electronic contribution. The complexes were characterized by multiple physical methods (¹H NMR, ¹³C NMR, FTIR, and UV-Vis spectroscopies, ESI-MS, and elemental analysis) to establish their structural properties. Moreover, the Re(I)-diimine complexes were analyzed using cyclic voltammetry in the absence and presence of CO₂ substrate to determine the impact of sterics and electronics on the electrochemical properties and electrocatalytic activity. In general, increasing the electronic contribution into the phenanthroline ligand from the 2 and 9 positions cathodically shifts the R₂phen- and Re-based redox couples, while increasing the steric bulk near the Re metal center increases the reversibility of the Re^{IV} oxidation. In both CH₃CN and DMF, the electronics appear to dominate the observed electrocatalytic CO₂ reduction activity with the electron-donating aryl-substituted complexes, **Re(Mes₂phen)**, **Re(2,4,6-tmp)₂phen)**, and **Re(3,4,5-tmp)₂phen)**, displaying increased current enhancement at more negative potentials with respect to the unsubstituted **Re(phen)** analogue. Interestingly, **Re((2,4,6-tmp)₂phen)** displayed a much higher current enhancement compared to the bulky **Re(Mes₂phen)** and **Re(3,4,5-tmp)₂phen)** catalysts in DMF solvent, but not in CH₃CN, indicating that solvent plays an important role in

catalysis. Ongoing studies in our lab include synthesizing and comparing the analogous hydroxyphenyl substituents to investigate the effect of intramolecular hydrogen bonding with weak Brønsted acids and a metallocarboxylate intermediate, as well as pursuing solvent effects on Re(I)-diimine electrocatalysts for CO₂ reduction.

Appendix A. Supplementary Information.

Supplementary data including HR-ESI(+)-MS data, ¹H NMR spectra, ¹³C NMR spectra, FTIR spectra, and cyclic voltammograms associated with this article can be found, in the online version, at

***Corresponding Author**

Mailing Address: Department of Chemistry & Biochemistry, 100 University Terrace, 136

Clippinger Laboratories, Athens, Ohio 45701, USA

E-mail address: whitet2@ohio.edu (T. A. White)

ORCID

Travis A. White: 0000-0002-6200-4416

Bertrand J. Neyhouse: 0000-0001-6747-8197

Author Contributions

The manuscript was written through contributions of all authors and all authors have given approval to the final version of the manuscript.

Notes

The authors declare no competing financial interest.

Declarations of interest: none

Acknowledgements

T.A.W. thanks Ohio University for start-up funds supporting this research. Acknowledgements are given to Mr. Brian Hivick (Prof. Hao Chen's research group, Ohio University) for his assistance with obtaining HR-ESI(+)-MS data, Prof. Howard Dewald (Ohio University) for assistance with bulk electrolysis electrodes, and Prof. Kyle Grice (DePaul University) for fruitful discussions.

References

- [1] G. Centi, S. Perathoner, *Catal. Today*, 148 (2009) 191.
- [2] E.E. Benson, C.P. Kubiak, A.J. Sathrum, J.M. Smieja, *Chem. Soc. Rev.*, 38 (2009) 89.
- [3] R. Francke, B. Schille, M. Roemelt, *Chem. Rev.*, (2018).
- [4] N. Elgrishi, M.B. Chambers, X. Wang, M. Fontecave, *Chem. Soc. Rev.*, 46 (2017) 761.
- [5] J.-M. Savéant, *Chem. Rev.*, 108 (2008) 2348.
- [6] M. Rakowski Dubois, D.L. Dubois, *Acc. Chem. Res.*, 42 (2009) 1974.
- [7] J. Rosenthal, Progress toward the electrocatalytic production of liquid fuels from carbon dioxide, in: K.D. Karlin (Ed.) *Progress in Inorganic Chemistry*, John Wiley & Sons, Inc.2014, pp. 299.
- [8] C. Costentin, M. Robert, J.-M. Savéant, *Acc. Chem. Res.*, 48 (2015) 2996.
- [9] J.D. Froehlich, C.P. Kubiak, *Inorg. Chem.*, 51 (2012) 3932.
- [10] J. Schneider, H. Jia, J.T. Muckerman, E. Fujita, *Chem. Soc. Rev.*, 41 (2012) 2036.
- [11] J. Schneider, H. Jia, K. Kobiro, D.E. Cabelli, J.T. Muckerman, E. Fujita, *Energy Environ. Sci.*, 5 (2012) 9502.
- [12] I. Azcarate, C. Costentin, M. Robert, J.-M. Savéant, *J. Amer. Chem. Soc.*, 138 (2016) 16639.
- [13] C. Costentin, S. Drouet, M. Robert, J.-M. Savéant, *Science*, 338 (2012) 90.
- [14] R.E. Cook, B.T. Phelan, L.E. Shoer, M.B. Majewski, M.R. Wasielewski, *Inorg. Chem.*, 55 (2016) 12281.
- [15] D.L. DuBois, A. Miedaner, R.C. Haltiwanger, *J. Amer. Chem. Soc.*, 113 (1991) 8753.
- [16] J.W. Raebiger, J.W. Turner, B.C. Noll, C.J. Curtis, A. Miedaner, B. Cox, D.L. DuBois, *Organometallics*, 25 (2006) 3345.
- [17] K.A. Grice, C.P. Kubiak, Recent Studies of Rhenium and Manganese Bipyridine Carbonyl Catalysts for the Electrochemical Reduction of CO₂, in: A. Michele, E. Rudi van (Eds.) *Advances in Inorganic Chemistry*, Academic Press2014, pp. 163.
- [18] J. Hawecker, J.-M. Lehn, R. Ziessel, *J. Chem. Soc. Chem. Commun.*, (1984) 328.
- [19] B.P. Sullivan, C.M. Bolinger, D. Conrad, W.J. Vining, T.J. Meyer, *J. Chem. Soc. Chem. Commun.*, (1985) 1414.
- [20] J.M. Smieja, C.P. Kubiak, *Inorg. Chem.*, 49 (2010) 9283.
- [21] M.L. Clark, P.L. Cheung, M. Lessio, E.A. Carter, C.P. Kubiak, *ACS Catal.*, 8 (2018) 2021.
- [22] A. Nakada, O. Ishitani, *ACS Catal.*, 8 (2018) 354.
- [23] C.W. Machan, J. Yin, S.A. Chabolla, M.K. Gilson, C.P. Kubiak, *J. Amer. Chem. Soc.*, 138 (2016) 8184.

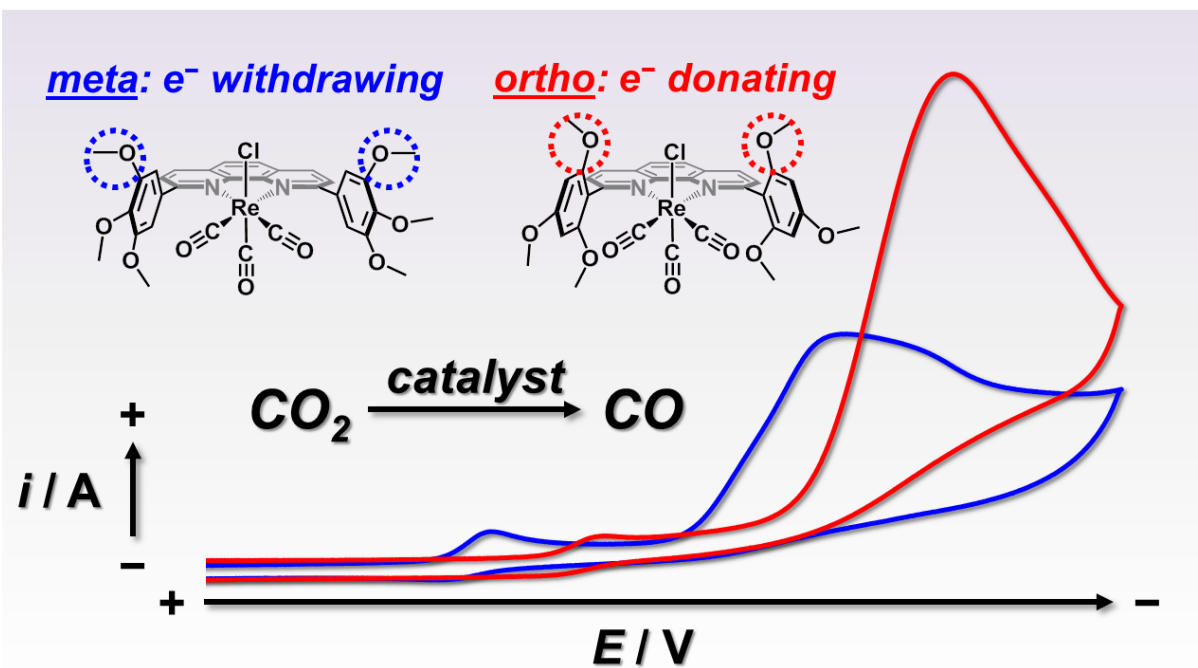
- [24] G.F. Manbeck, J.T. Muckerman, D.J. Szalda, Y. Himeda, E. Fujita, *J. Phys. Chem. B*, 119 (2015) 7457.
- [25] C.W. Machan, S.A. Chabolla, J. Yin, M.K. Gilson, F.A. Tezcan, C.P. Kubiak, *J. Amer. Chem. Soc.*, 136 (2014) 14598.
- [26] S.A. Chabolla, E.A. Dellamary, C.W. Machan, F.A. Tezcan, C.P. Kubiak, *Inorg. Chim. Acta*, 422 (2014) 109.
- [27] J.J. Teesdale, A.J. Pistner, G.P.A. Yap, Y.-Z. Ma, D.A. Lutterman, J. Rosenthal, *Catalysis Today*, 225 (2014) 149.
- [28] E. Portenkirchner, K. Oppelt, C. Ulbricht, D.A.M. Egbe, H. Neugebauer, G. Knör, N.S. Sariciftci, *J. Organomet. Chem.*, 716 (2012) 19.
- [29] K.A. Grice, N.X. Gu, M.D. Sampson, C.P. Kubiak, *Dalton Trans.*, 42 (2013) 8498.
- [30] D.H. Gibson, X. Yin, H. He, M.S. Mashuta, *Organometallics*, 22 (2003) 337.
- [31] D.H. Gibson, X. Yin, *Chem. Commun.*, (1999) 1411.
- [32] D.H. Gibson, X. Yin, *J. Amer. Chem. Soc.*, 120 (1998) 11200.
- [33] M.D. Sampson, J.D. Froehlich, J.M. Smieja, E.E. Benson, I.D. Sharp, C.P. Kubiak, *Energy Environ. Sci.*, 6 (2013) 3748.
- [34] F.P.A. Johnson, M.W. George, F. Hartl, J.J. Turner, *Organometallics*, 15 (1996) 3374.
- [35] A. Wilting, T. Stolper, R.A. Mata, I. Siewert, *Inorg. Chem.*, 56 (2017) 4176.
- [36] S. Sung, D. Kumar, M. Gil-Sepulcre, M. Nippe, *J. Amer. Chem. Soc.*, 139 (2017) 13993.
- [37] F. Franco, C. Cometto, L. Nencini, C. Barolo, F. Sordello, C. Minero, J. Fiedler, M. Robert, R. Gobetto, C. Nervi, *Chem. Eur. J.*, 23 (2017) 4782.
- [38] J. Agarwal, T.W. Shaw, H.F. Schaefer, A.B. Bocarsly, *Inorg. Chem.*, 54 (2015) 5285.
- [39] F. Franco, C. Cometto, F. Ferrero Vallana, F. Sordello, E. Priola, C. Minero, C. Nervi, R. Gobetto, *Chem. Commun.*, 50 (2014) 14670.
- [40] K.T. Ngo, M. McKinnon, B. Mahanti, R. Narayanan, D.C. Grills, M.Z. Ertem, J. Rochford, *J. Amer. Chem. Soc.*, 139 (2017) 2604.
- [41] S. Sinha, E.K. Berdichevsky, J.J. Warren, *Inorg. Chim. Acta*, 460 (2017) 63.
- [42] J.K. Nganga, C.R. Samanamu, J.M. Tanski, C. Pacheco, C. Saucedo, V.S. Batista, K.A. Grice, M.Z. Ertem, A.M. Angeles-Boza, *Inorg. Chem.*, 56 (2017) 3214.
- [43] Y. Liang, M.T. Nguyen, B.J. Holliday, R.A. Jones, *Inorg. Chem. Commun.*, 84 (2017) 113.
- [44] C.J. Stanton, C.W. Machan, J.E. Vandezande, T. Jin, G.F. Majetich, H.F. Schaefer, C.P. Kubiak, G. Li, J. Agarwal, *Inorg. Chem.*, 55 (2016) 3136.
- [45] N.P. Liyanage, H.A. Dulaney, A.J. Huckaba, J.W. Jurss, J.H. Delcamp, *Inorg. Chem.*, 55 (2016) 6085.
- [46] H.Y.V. Ching, X. Wang, M. He, N. Perujo Holland, R. Guillot, C. Slim, S. Griveau, H.C. Bertrand, C. Policar, F. Bedioui, M. Fontecave, *Inorg. Chem.*, 56 (2017) 2966.
- [47] X. Qiao, Q. Li, R.N. Schauggaard, B.W. Noffke, Y. Liu, D. Li, L. Liu, K. Raghavachari, L.-s. Li, *J. Amer. Chem. Soc.*, 139 (2017) 3934.
- [48] B. Rezaei, M. Mokhtarianpour, H. Hadadzadeh, A.A. Ensafi, J. Shakeri, *J. CO₂ Util.*, 16 (2016) 354.
- [49] F. Franco, C. Cometto, C. Garino, C. Minero, F. Sordello, C. Nervi, R. Gobetto, *Eur. J. Inorg. Chem.*, 2015 (2015) 296.
- [50] A. Bencini, V. Lippolis, *Coord. Chem. Rev.*, 254 (2010) 2096.
- [51] R.M. Bullock, A.K. Das, A.M. Appel, *Chem. Eur. J.*, 23 (2017) 7626.
- [52] S. Oh, J.R. Gallagher, J.T. Miller, Y. Surendranath, *J. Amer. Chem. Soc.*, 138 (2016) 1820.

- [53] M.N. Jackson, S. Oh, C.J. Kaminsky, S.B. Chu, G. Zhang, J.T. Miller, Y. Surendranath, J. Amer. Chem. Soc., 140 (2018) 1004.
- [54] L. Kohler, D. Hayes, J. Hong, T.J. Carter, M.L. Shelby, K.A. Fransted, L.X. Chen, K.L. Mulfort, Dalton Trans., 45 (2016) 9871.
- [55] G.R. Fulmer, A.J.M. Miller, N.H. Sherden, H.E. Gottlieb, A. Nudelman, B.M. Stoltz, J.E. Bercaw, K.I. Goldberg, Organometallics, 29 (2010) 2176.
- [56] U. Lüning, M. Abbass, F. Fahrenkrug, Eur. J. Org. Chem., 2002 (2002) 3294.
- [57] D.M. Dattelbaum, R.L. Martin, J.R. Schoonover, T.J. Meyer, J. Phys. Chem. A, 108 (2004) 3518.
- [58] A.M. Blanco-Rodriguez, M. Towrie, J.-P. Collin, S. Zalis, A.V. Jr, Dalton Trans., (2009) 3941.
- [59] M. Wrighton, D.L. Morse, J. Amer. Chem. Soc., 96 (1974) 998.
- [60] A. Wozna, A. Kapturkiewicz, Phys. Chem. Chem. Phys., 17 (2015) 30468.
- [61] K. Kalyanasundaram, J. Chem. Soc., Faraday Trans. 2, 82 (1986) 2401.
- [62] F. Paolucci, M. Marcaccio, C. Paradisi, S. Roffia, C.A. Bignozzi, C. Amatore, J. Phys. Chem. B, 102 (1998) 4759.
- [63] J.P. Bullock, E. Carter, R. Johnson, A.T. Kennedy, S.E. Key, B.J. Kraft, D. Saxon, P. Underwood, Inorg. Chem., 47 (2008) 7880.
- [64] A.H. Said, F.M. Mhalla, C. Amatore, L. Thouin, C. Pebay, J.-N. Verpeaux, J. Electroanal. Chem., 537 (2002) 39.
- [65] E.S. Rountree, B.D. McCarthy, T.T. Eisenhart, J.L. Dempsey, Inorg. Chem., 53 (2014) 9983.

Highlights:

- New Re(I)-phenanthroline electrocatalysts for CO₂ reduction were synthesized
- Substituent modifications indicate electronics dominate observed catalytic activity
- CH₃CN and DMF solvents display varying degrees of catalytic enhancement

ACCEPTED MANUSCRIPT



ACCEPTED MA